

# Morphology and gas permselectivity of blend membranes of polyvinylpyridine with ethylcellulose

Xin-Gui Li<sup>a,b,\*</sup>, Ingo Kresse<sup>b</sup>, Jürgen Springer<sup>b</sup>, Jörg Nissen<sup>c</sup>, Yu-Liang Yang<sup>d</sup>

<sup>a</sup>Department of Polymer Materials Science and Engineering, College of Materials Science and Engineering, Tongji University, 1239 Siping Road, Shanghai 200092, People's Republic of China

<sup>b</sup>Macromolecular Chemistry, Institute of Technical Chemistry, Technical University of Berlin, D-10623 Berlin, Germany

<sup>c</sup>Zentraleinrichtung Elektronenmikroskopie, Technical University of Berlin, D-10623 Berlin, Germany

<sup>d</sup>Department of Macromolecular Science, Key Laboratory of Molecular Engineering of Polymers, Fudan University, Shanghai 200433, People's Republic of China

Received 23 October 2000; received in revised form 21 December 2000; accepted 9 January 2001

## Abstract

Binary blend membranes of poly(4-vinylpyridine) (PVP) with ethylcellulose (EC) have been prepared by a solution casting technique with chloroform as solvent. The membranes appear macroscopically miscible but microscopically immiscible based on wide-angle X-ray diffraction, differential scanning calorimetry and scanning electron microscope investigations. Permeating feature of five pure gases through the blend membranes has been described in detail. The permeability, diffusivity, solubility, and their selectivities of oxygen, nitrogen, carbon dioxide, methane and hydrogen through the blend membranes have been measured over an entire range of blend composition in a time-lag apparatus. A remarkably and continuously enhanced selectivity has been achieved for important gas pairs including oxygen/nitrogen, carbon dioxide/methane, and hydrogen/nitrogen with increasing PVP content from zero to 100 wt%. The highest oxygen over nitrogen, carbon dioxide over methane, and hydrogen over nitrogen selectivity coefficients are, respectively, equal to 6.8, 25, and 70. Experimental permeability was compared with that calculated on the basis of blend composition. The various transport parameters of the five gases through the blends seem normally higher than composition weighted mean computed from pure PVP and pure EC values using semilogarithmic coordinates. The temperature- and pressure-dependences of the permeability of the five gases through a PVP/EC (50/50) blend membrane are discussed. © 2001 Elsevier Science Ltd. All rights reserved.

**Keywords:** Blend morphology; Poly(4-vinylpyridine)/ethylcellulose blend membrane; Gas permselectivity

## 1. Introduction

Permselectivity of gas through a polymer blend has been the subject of numerous investigations [1–8]. Gas separation membranes prepared by blending are of great interest and importance because a useful combination of the advantage of each polymer into a new product can be achieved and a continuous range of performances can be expected by controlling blend composition and micro- and macrostructure. Furthermore, the blending of polymers can result in properties not found in a single polymer. Gas permselectivity through miscible polymer blends is reported to vary monotonically between those of the pure polymers.

However, the permselectivity through immiscible blend membranes strongly depends on their morphology: the volume fraction and the size and shape of the dispersed and continuous phases. The relationship between their volume fraction and permselectivity through the incompatible blend membranes has been widely studied.

However, the influence of the size and shape of dispersed phase has not been paid much attention [9]. Ethylcellulose (EC) has been believed as a kind of polymer material with better membrane-forming ability, good flexibility, medium gas-separation capability, and low cost [3–8]. Poly(4-vinylpyridine) (PVP) possesses a good gas permselectivity [7,10]. It should be noted that PVP is very brittle and strongly adheres to the most solid surfaces, from which it is not possible to remove the membrane easily, in order to form a free-standing membrane. As a matter of fact, the ability of PVP to form a flexible thin film is very bad. Therefore, a blend membrane prepared from PVP with EC could overcome the strong adhesion with the most solid surfaces

\* Corresponding author. Present address: Department of Polymer Materials Science and Engineering, College of Materials Science and Engineering, Tongji University, 1239 Siping Road, Shanghai 200092, People's Republic of China. Tel.: +86-21-65799455; fax: +86-21-65982461.

E-mail address: [lixingui@citiz.net](mailto:lixingui@citiz.net) (X.-G. Li).

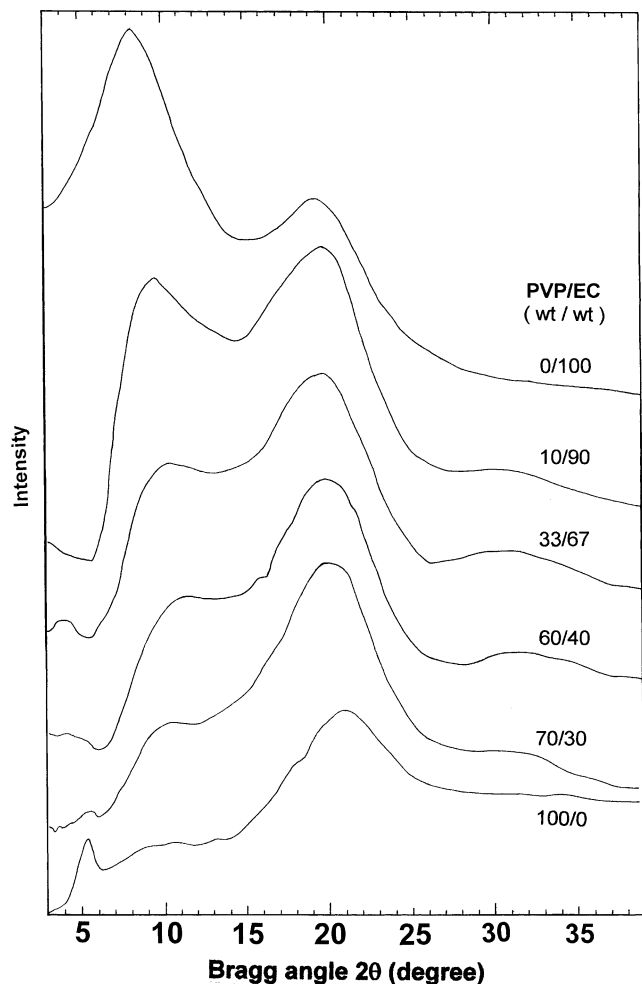


Fig. 1. Wide-angle X-ray diffraction diagrams of the blend membranes made of poly(4-vinylpyridine) (PVP)/ ethylcellulose (EC) with PVP/EC weight ratios from top to bottom: 0/100, 10/90, 33/67, 60/40, 70/30, 100/0.

as well as the brittleness of PVP, and enhance the gas permselectivity of EC at the same time. However, little report concerning the preparation of the PVP/EC blend membrane was found. Furthermore, no data about the gas permselectivity through the blend membrane were reported in literature.

The objective of this work is to prepare free-standing binary blend membranes of PVP with EC, to investigate the membrane morphology including the domain size and shape, permeability, diffusivity, and solubility of five gases through the membrane, and to elaborate the variation of its permeability, diffusivity, solubility, and their selectivities with blend composition and morphology.

## 2. Experimental

### 2.1. Materials

Linear PVP particle of average  $M_w \sim 160,000$  g/mol with

$T_g$  142°C was purchased from Aldrich Chemical Company, (Milwaukee WI 53233 USA). EC particle produced by Shantou Xinning Chemical Works of Guangdong Province in China has the viscosity 0.05–0.07 Pa s measured in ethanol/toluene at 25°C. The degree of substitution of the EC is about 2.4. Oxygen (99.99%), nitrogen (99.99%), carbon dioxide (99.99%), methane (99.5%), and hydrogen (99.99%) were obtained from Messer Griesheim GmbH, Duesseldorf, Germany. PVP, EC, five pure gases, and chloroform were directly used without any purification.

### 2.2. Membrane preparation

The PVP and EC particles of 0.3 g were dissolved in 5 ml chloroform to form a 6 wt% solution. The polymer solution was poured into a Petri dish made in Germany. Solvent was allowed to evaporate slowly from the solution at 25°C and 60% relative humidity for ca. 20 h. The resultant membrane was removed from the Petri dish by pouring some water and dried in a high vacuum at 45°C for another 4 h. The blend membrane is flexible to some extent and has the thickness of 100–110  $\mu\text{m}$ .

### 2.3. Morphology characterization

The PVP/EC blend membranes were characterized by Fourier wide-angle X-ray diffraction (WAXD) in a range of Bragg angle 3–50° using the wave length 0.154 nm of  $\text{CuK}\alpha$  electron beam in step-by-step scanning region and recorded nickel filtered radiation at 25°C with a Bruker Analytical X-ray Systems D8 Advance X-ray Diffractometer made in Germany. The scanning rate is 2°/min.

Perkin–Elmer DSC 7 thermal analytical system was used to measure the glass transition temperature of the PVP/EC blend membranes at a heating rate of 10°C/min and a cooling rate of –10°C/min with the sample size of 3–6 mg.

The morphology of the PVP/EC blend membranes was observed by scanning electron microscope (SEM) Hitachi S-2700 made in Japan. The blend membranes were etched by immersing the membranes into 30 vol% ethanol aqueous solution for about 3 h. The PVP component in the membranes was dissolved but EC component did not dissolve or swell at all. Therefore the surface of the residual solid sample should consist of the EC phase. Before the SEM observation, all the samples should be coated with 15 nm gold layer in order to enhance the electrical conductivity of the samples and furthermore the resolution of the microphotographs.

### 2.4. Gas permeation measurements

The gas permeation performance of the PVP/EC blend membranes was measured using a constant volume, variable pressure approach with a self-built vacuum time-lag apparatus [11]. After both sides of a membrane were evacuated, the pure gas was introduced to the upstream side of the membrane, and was allowed to permeate to the downstream

Table 1  
 Characteristics of the blend membranes of poly(4-vinylpyridine) (PVP) with ethylcellulose (EC) determined by wide-angle X-ray diffraction and differential scanning calorimetry

PVP/EC (wt/wt)	0/100	10/90	22/78	33/67	50/50	60/40	70/30	100/0
Diffraction angle (degree)	8.1, 19.1	9.2, 19.3	–	4.1, 10.4, 19.3	–	4.3, 10.4, 20.0	5.1, 10.5, 20.0	5.2, 10.9, 20.6
<i>d</i> -Spacing (nm)	1.11, 0.46	0.96, 0.46	–	2.16, 0.85, 0.46	–	2.06, 0.84, 0.44	1.73, 0.83, 0.44	1.7, 0.81, 0.43
<i>T<sub>g</sub></i> (°C) determined by heating curves	60	169	183	175	60, 170	170	155	182
<i>T<sub>g</sub></i> (°C) determined by cooling curves	75	–	100	100	100 <sup>a</sup>	–	–	140
Membrane appearance	Transparent	Transparent	Basically transparent	Slightly foggy	Turbid	Turbid	Turbid	Turbid
Membrane flexibility	Flexible	Very flexible	Very flexible	Flexible	Flexible	Slightly brittle	Brittle	Very brittle

<sup>a</sup> Very weak transition.

side at an initial pressure of 0.01 mbar. After a certain period of time, a steady state was reached at which the amount of gas permeated increased linearly with time. An increase in permeate pressure with time was recorded by two pressure sensors (10 mbar maximum (downstream side), 20 bar maximum (upstream side)) that were connected directly to a computer. The software used ensures automated measurement with an automatically adapting data-sampling rate to yield at least 600 data points and to describe time-lag and steady-state gas transport completely. The permeability coefficient, *P*, was calculated from the slope of the straight line in the steady-state region. Apparent diffusion coefficient, *D*, was estimated from the time-lag  $\tau$  by  $D = l^2/6\tau$  (*l* being the membrane thickness). Apparent solubility coefficient, *S*, was calculated from  $S = P/D$ . When the downstream pressure is negligible relative to the upstream pressure, the ideal separation factor of a membrane for a gaseous mixture of A and B can be related simply to a ratio ( $P_A/P_B$ ) of two permeabilities of A and B. Diffusion selectivity and solubility selectivity were defined as  $D_A/D_B$  and  $S_A/S_B$ , respectively. The experimental errors vary with the magnitudes of the permeability and time lag and are about 5% for O<sub>2</sub>, CO<sub>2</sub>, and H<sub>2</sub>, and about 10% for N<sub>2</sub> and CH<sub>4</sub>.

### 3. Results and discussion

#### 3.1. Blend morphology

The phase morphology of the PVP/EC blend membranes has been investigated by using WAXD, DSC, and SEM. The WAXD diagrams shown in Fig. 1 suggest that the blend membranes are amorphous. Two major diffraction peaks shift slowly and slightly to larger Bragg angle with increasing PVP content. That is to say, the corresponding *d*-spacings become smaller, as listed in Table 1. This implies a more compact structure or more efficient packing. The strongest peak for pure EC membrane becomes weaker while the weaker peak for the EC membrane becomes the strongest with an increase in PVP content. An additional and sharp diffraction peak at a small angle of 5.2° observed for pure PVP membrane becomes weaker and broader for PVP/EC blend membranes. These point to a local phase-separation in the PVP/EC blend membranes. In fact, all the blend and pure PVP membranes exhibit the strongest diffraction peak at a larger Bragg angle, implying that they have more compact structure than pure EC. These can be used to explain lower gas permeability but higher separation factor than pure EC, as discussed below.

The heating and cooling DSC curves of the PVP/EC blend membranes are shown in Figs. 2 and 3. The results of the calorimetric studies concerning the phase state of the blend membranes were listed in Table 1. All blends were heated from ambient temperature to 300°C at a heating rate of 10°C/min, and maintained at 300°C for about 30 min, and

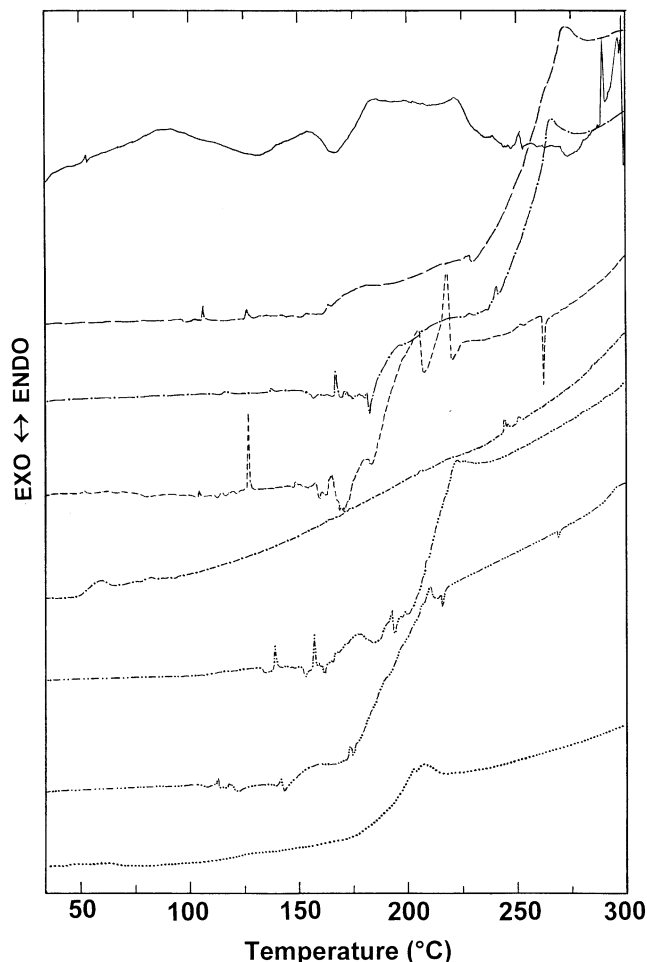


Fig. 2. Differential scanning calorimetry thermograms of the blend membranes made of poly(4-vinylpyridine) (PVP)/ethylcellulose (EC) with PVP/EC weight ratios (from the top to the bottom) of (a) 0/100 (—), (b) 10/90 (---), (c) 22/78 (— · — · —), (d) 33/67 (- - - -), (e) 50/50 (- · - · -), (f) 60/40 (- · · · ·), (g) 70/30 (- · · · · ·), and (h) 100/0 (· · · · ·) at a heating rate of 10°C/min.

then cooled from 300°C to ambient temperature. It is found that the glass transition temperatures ( $T_g$ ) of the blends fall between two  $T_g$  values of the pure polymers based on heating and cooling curves although no thermal transition peaks are observed in some cooling DSC curves. For the PVP/EC (50/50) blend membrane, a very broad and weak transition range centered at about 170°C appears to be observed and accompanies with an additional, lower and narrower glass transition temperature at 60°C, which is corresponding to pure EC component. This is an indication of biphasic structure in the PVP/EC (50/50) blend membrane.

As-prepared PVP/EC blend membranes look homogeneous and smooth but turbid with a naked eye. The turbid appearance of the blends is due to the PVP component because pure PVP membrane is turbid at room temperature, whereas the pure EC membrane is transparent, as listed in Table 1. The morphology of the blends etched by 30% ethanol aqueous solution was investigated by SEM. In this

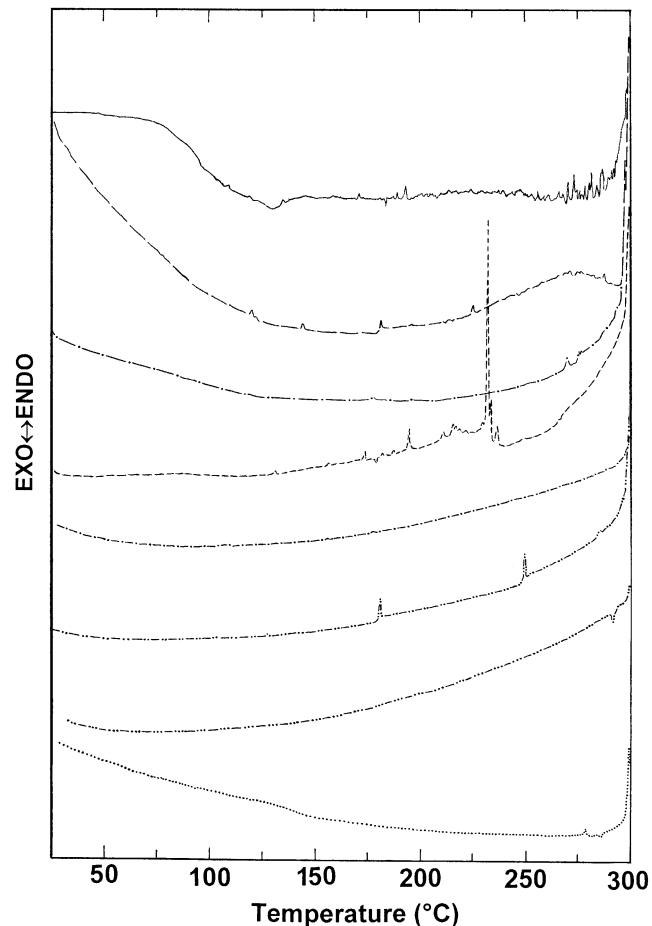


Fig. 3. Differential scanning calorimetry thermograms of the blend membranes made of poly(4-vinylpyridine) (PVP)/ethylcellulose (EC) with PVP/EC weight ratios of (a) 0/100 (—), (b) 10/90 (---), (c) 22/78 (— · — · —), (d) 33/67 (- - - -), (e) 50/50 (- · - · -), (f) 60/40 (- · · · ·), (g) 70/30 (- · · · · ·), and (h) 100/0 (· · · · ·) at a cooling rate of 10°C/min.

aqueous solution only PVP component was dissolved. After the blend membranes were etched, washed with water, and dried, they can scatter light and look quite different from the non-etched membranes. These phenomena imply the formation of porous structure in the membranes. Representative SEM photographs of the etched PVP/EC (22/78), (33/67), and (50/50) membranes are shown in Fig. 4. Apparently, EC component is a continuous phase, whereas PVP is a discontinuous phase when PVP content is lower than 50 wt%. These PVP/EC blends consist of the continuous phase into which the PVP phase is dispersed. Actually, based on a comparison of Fig. 4(a) and (b) with Fig. 4(c), with an increase in PVP content from 22 to 50 wt%, the porosity and roughness on the membrane surface and section increase steadily and the hole size and number become larger. Consequently, it can be believed that the domain size and number of dispersed PVP phase are increased with the increase of PVP content. In the case of the PVP/EC (50/50) membrane (Fig. 4(c)), the PVP domains are particles of regular shape, roughly equivalent to ellipsoids,

spheroid, and spheres. The PVP spheroid has various sizes and distributes randomly in the EC matrix with a rough surface that implies an interaction between PVP and EC phases to some extent. The large spheroid is less and has the largest diameter of 45  $\mu\text{m}$ . More PVP spheroids are much smaller and their diameters are about 6  $\mu\text{m}$ . There is some possibility of forming continuous PVP paths from one side to another side of the PVP/EC (50/50) membrane on the basis of a close observation of Fig. 4(c). It seems that there is an interpenetrating bicontinuous phase consisting of a mainly continuous EC phase and a subordinately continuous PVP phase. That is to say, the phase inversion may occur when PVP content increased up to 50 wt%. These give rise to the decreased permeability but enhanced selectivity, as discussed below. It was reported that a phase inversion of immiscible blend membrane made of polyphenyleneoxide and polyisoprene also occurred at the weight ratio of 50/50 [9].

### 3.2. Gas permeation performance

Fig. 5 exhibits the variation of downstream pressure of five pure gases through the PVP/EC (60/40) blend membrane with time at 25°C. Five gases permeate the membrane in different ways. Apparently,  $\text{H}_2$  with the smallest molecular size permeates the membrane at the fastest rate with the shortest time-lag of 7 s, while  $\text{CO}_2$  also permeates the membrane very rapidly after a long time-lag of 830 s.  $\text{CH}_4$  with the largest molecular size exhibits the slowest permeation rate through the membrane with the longest time-lag of 2730 s.

As a new blend membrane, it is necessary to investigate the gas permeability and permselectivity through the PVP/EC blend membranes. As shown in Fig. 6, with increasing PVP content, the permeability of all five gases through the membranes at 25°C decreases but the permselectivity increases. Note that  $P_{\text{O}_2}$ ,  $P_{\text{CO}_2}$ , and  $P_{\text{CH}_4}$  decreased faster but  $P_{\text{CO}_2}/P_{\text{CH}_4}$  and  $P_{\text{H}_2}/P_{\text{N}_2}$  increased faster in a range of PVP content from 50 to 60 wt%. These behaviors may be owing to a faster increase in continuous PVP phase, that provides a continuous PVP path verified by SEM observation (Fig. 4(c)). Perhaps, the gas permselectivity through the PVP/EC blend membranes is controlled by PVP component, when PVP content is higher than 50 wt%. In fact, the mechanical property of PVP/EC is controlled by PVP phase if the PVP content is higher than 50 wt% because the PVP/EC blend membranes having 60 wt% PVP or more are brittle just like pure PVP, as shown in Table 1, whereas the PVP/EC blend membranes having 50 wt% PVP or less are flexible just like pure EC. The highest  $P_{\text{O}_2}/P_{\text{N}_2}$ ,  $P_{\text{CO}_2}/P_{\text{CH}_4}$ , and  $P_{\text{H}_2}/P_{\text{N}_2}$  for PVP/EC blend membranes are 6.8, 25, and 70 respectively, which are much higher than those through pure EC membrane. The great enhancement of the gas permselectivity through PVP/EC membranes should be attributed to the PVP component. Apparently, the PVP/EC blend prepared by a simple solution blending

method exhibits higher oxygen/nitrogen separation factor than some polyimide ( $P_{\text{O}_2}/P_{\text{N}_2} = 6.2$ ) and polypyrrolone ( $P_{\text{O}_2}/P_{\text{N}_2} = 6.5$ ), which were prepared by a more complicated and difficult process [7].

The permeability coefficients for the PVP/EC membranes containing less than 25 wt% PVP component increase in the order of gases

$$P_{\text{N}_2} < P_{\text{CH}_4} < P_{\text{O}_2} < P_{\text{H}_2} < P_{\text{CO}_2}$$

For the PVP/EC membranes containing more than 25 wt% PVP component,  $P_{\text{CO}_2} < P_{\text{H}_2}$ . As discussed below,  $S_{\text{CO}_2}$  is large but  $D_{\text{CO}_2}$  is small, and  $S_{\text{H}_2}$  is small but  $D_{\text{H}_2}$  is large, as the result  $P_{\text{H}_2} < \text{or} > P_{\text{CO}_2}$ . The highest  $P_{\text{H}_2}$  should be due to the highest diffusivity of  $\text{H}_2$  (the smallest molecular diameter) regardless of its lowest solubility. It could be concluded that the PVP/EC blend membranes are more permeable to  $\text{CO}_2$  than  $\text{H}_2$  at the PVP content of less than 25 wt%. On the contrary, the blends are more permeable to hydrogen than carbon dioxide in a PVP content range from 25 to 100 wt%. Possible reason is that the more PVP-containing membranes possess denser structure. One of evidences is that pure PVP membrane exhibits much lower gas permeability [10] than pure EC [3–8].

The straight and short dash lines in Fig. 6 are corresponding to the calculated results for weakly interacting blends based on the following a logarithmic additivity rule:

$$\ln P = w_A \ln A + w_B \ln B \quad (1)$$

where  $w_A$  and  $w_B$  are the weight fractions of two pure polymers. Because the density of pure EC of 1.14  $\text{g}/\text{cm}^3$  is nearly the same as the density of pure PVP of 1.15  $\text{g}/\text{cm}^3$ , the Eq. (1) was deduced from the following Eq. (2) [12]:

$$\ln P = v_A \ln A + v_B \ln B \quad (2)$$

where  $v_A$  and  $v_B$  are the volume fractions of two pure polymers. The experimental and calculated oxygen permeabilities based on Eq. (1) are almost the same. The oxygen permeability of the membranes varies linearly between the permeability values of the pure polymer components, in accordance with polymer mixing theory in homogeneous systems. The deviations from this rule for the other four gas permeabilities through the PVP/EC blend membranes are smaller than those calculated by other equations reviewed in Ref. [13]. Note that the experimental permeability through the blend membranes is larger than that calculated by Eq. (1) in a range of the PVP content from 10 to 50 wt%. It was reported that gas permeability through the miscible blends is slightly lower than predicted by the ideal semilogarithmic mixing rule and that through the immiscible blends is higher [2]. Thus, it can be concluded that the PVP and EC are incompatible microscopically. At this scale, they form a two-phase system with weak interaction. Furthermore, EC component prevails and determines the gas permeation property of the PVP/EC blend membranes in a PVP content from zero to 50 wt%. In any

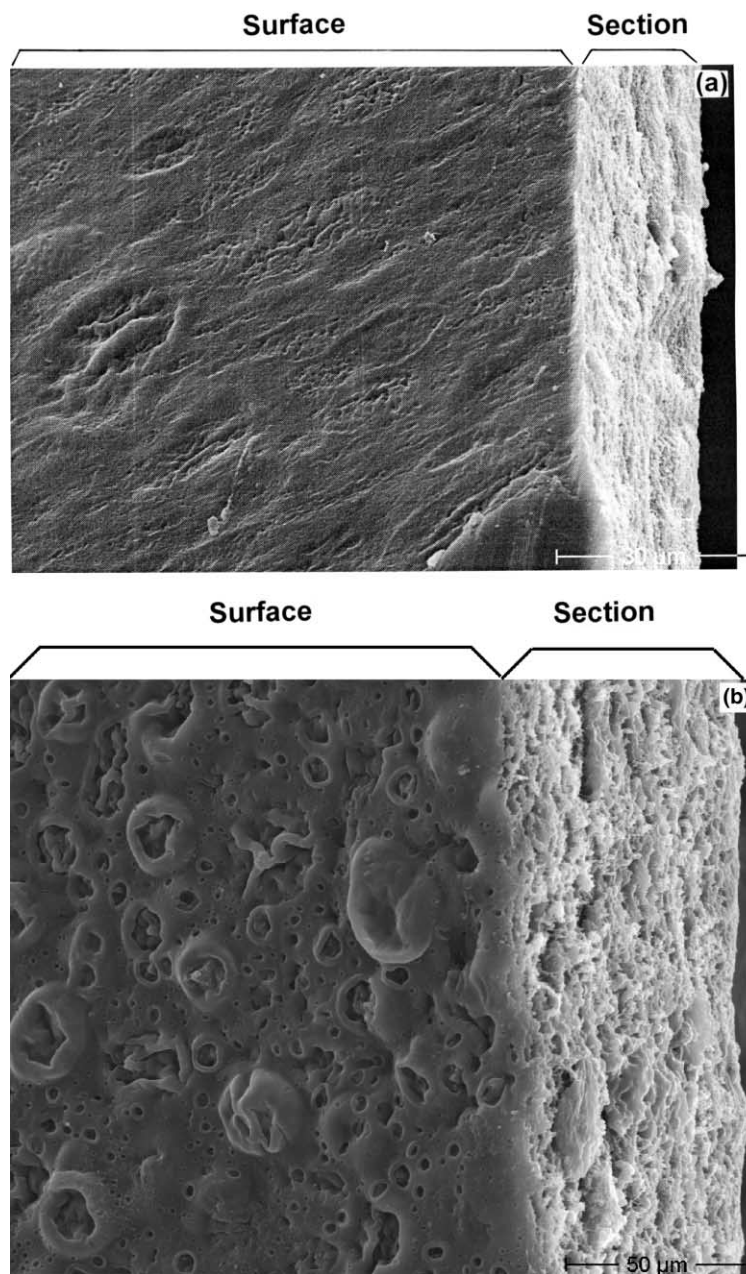


Fig. 4. SEM photographs of the ethanol etched blend membranes made of poly(4-vinylpyridine) (PVP)/ethyl cellulose (EC) with three PVP/EC weight ratios of (a) 22/78, (b) 33/67, and (c) 50/50.

case, these results in Fig. 6 show a significant correlation between the permeability and the composition for new microscopically phase-separated polymer blends. These conclusions are in general agreement with results of the gas permeability through the immiscible blend membranes of polyvinyl chloride and ethylene-vinyl acetate copolymer [14], whereas miscible blend membranes exhibit negative deviation of permeability and diffusion coefficients from simple logarithmic additive relations, which were observed and interpreted as a result of the decrease in volume on mixing of the blends, such as polycarbonate–polymethyl methacrylate blend [2], polycarbonate–poly (1,4-cyclo-

hexanedimethanol terephthalate/isophthalate (80/20)) blend [15], and polyphenyleneoxide–polystyrene blend [16].

It can be seen from Fig. 6 that the three permselectivities for three gas pairs increase linearly first and then exhibit an abrupt jump with increasing PVP content. This permselectivity jump corresponds to a PVP content range from 50 to 60 wt%. One of reasons is that a coherent phase of PVP decreases the permeability but increases the permselectivity sharply. The inversion from EC to PVP as coherent phase in the blend membranes might occur at 50 wt% of PVP in the blends. It should be noted that the PVP/EC blend dense membranes can withstand high temperature (55°C) and

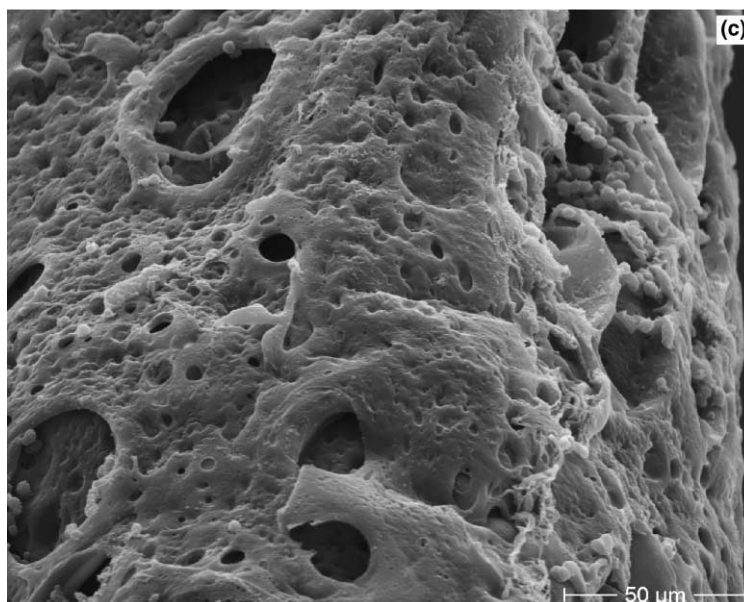


Fig. 4. (continued)

very high pressure difference (20 bar) for a long period of time without any membrane destructure and permselectivity loss [18]. This observed behavior might have practical utility when good performance stability is an issue.

### 3.3. Gas diffusion performance

The gas diffusivity through the PVP/EC blend membranes at 25°C are shown in Fig. 7. The diffusivity of

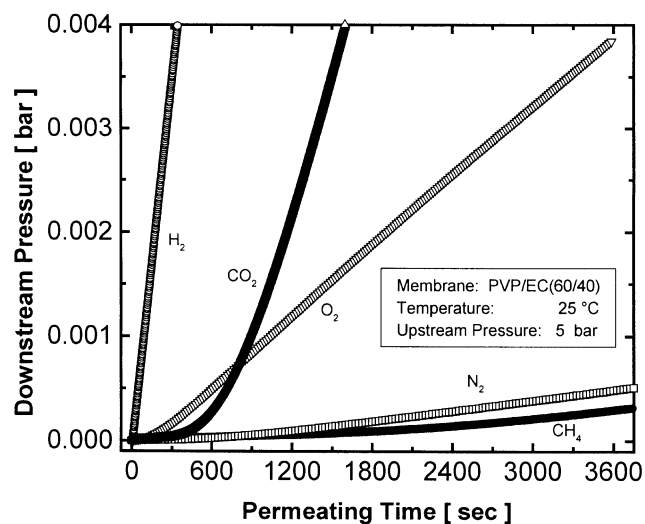


Fig. 5. Relationship between the downstream pressure and permeating time for oxygen, nitrogen, carbon dioxide, methane, and hydrogen permeation through the poly(4-vinylpyridine) (PVP)/ethyl cellulose (EC) blend membrane with a PVP/EC weight ratio of 60/40 at the upstream pressure 5 bar at 25°C.

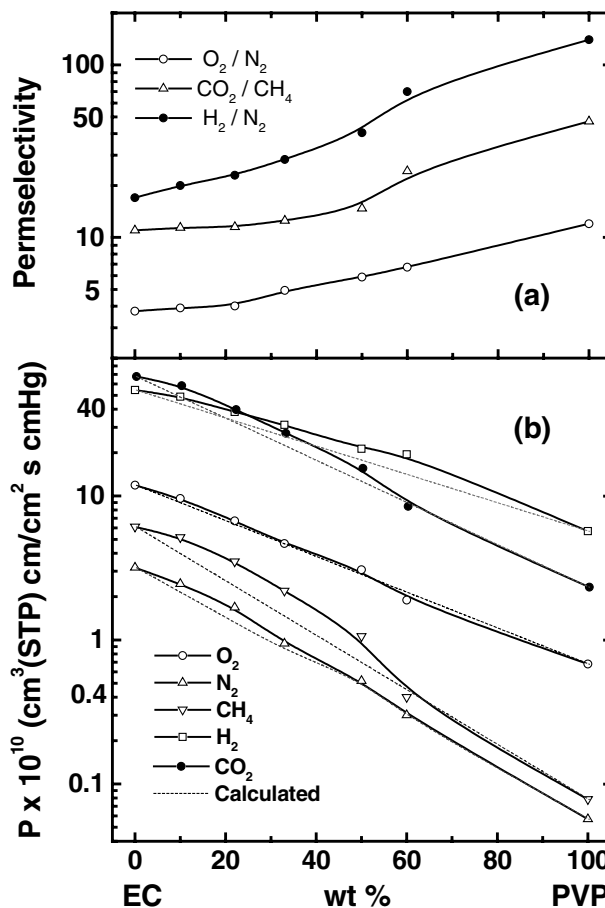


Fig. 6. The variation of permeability (b) and permeability selectivity (a) through the blend membranes of poly(4-vinylpyridine) (PVP)/ethyl cellulose (EC) with blend composition at 25°C and transmembrane pressure difference of 1–5 bar.

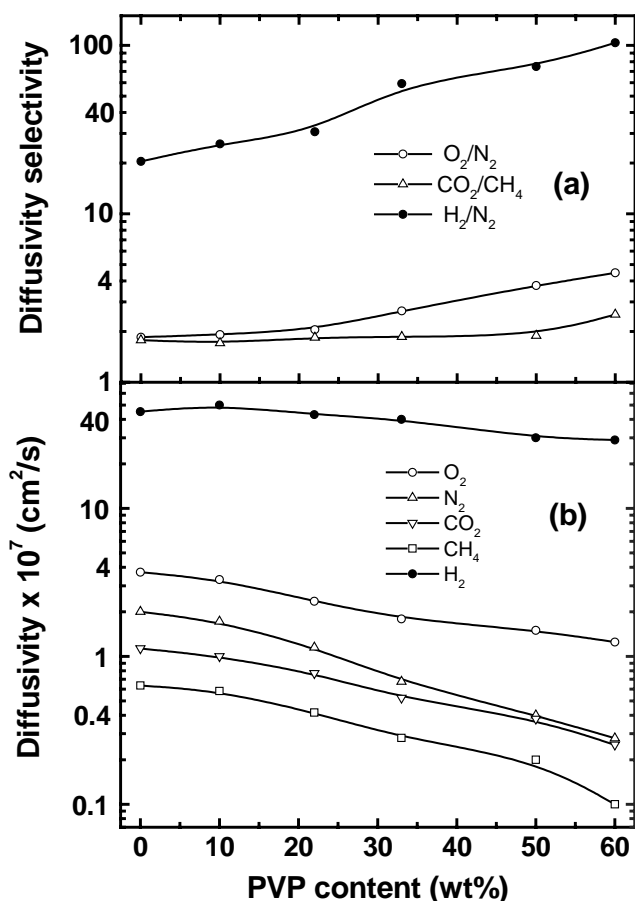


Fig. 7. The variation of diffusivity (b) and diffusivity selectivity (a) through the blend membranes of poly(4-vinylpyridine) (PVP)/ethyl cellulose (EC) with PVP content at 25°C and transmembrane pressure difference of 1–5 bar.

five gases through the blend membranes decreases monotonically with increasing PVP content from zero to 60 wt%. On the contrary, the diffusivity selectivity of three gas pairs increases with increasing PVP content. The same variations of permeability and permselectivity with blend composition have been observed in Fig. 6 and discussed above. Except that the diffusivity of  $O_2$  through the blend membranes versus weight percent of PVP approaches logarithmic linearity, positive deviation of diffusion coefficients for other four gases from simple logarithmic additive relations is observed and interpreted as a result of the increase in volume on mixing of the blends. As compared with the diffusion coefficients from simple logarithmic additivity, slightly higher experimental diffusivity suggests that the PVP/EC blends are microscopically phase-separation because the diffusion coefficients through the miscible blends should be smaller than from simply logarithmic additivity [2].

It should be noted that the  $H_2$  diffusion is much greater than those of other four gases through the membranes, leading much higher diffusion selectivity of  $H_2$  over  $N_2$ . A reason is that  $H_2$  has the smallest effective diameter of the

molecule and the weakest interaction with the blends. Smaller diffusivity of  $CO_2$  through the blend membranes is attributed to the relatively high solubility and a nonspherical molecular shape especially the strong interacting of  $CO_2$  with the blend membranes. The interaction hinders the mobility of  $CO_2$  molecule through the blends. Therefore, it is seen from Fig. 7 that the trend of the diffusion coefficients for five gases is quite different from the permeability coefficients as follows:

$$D_{CH_4} < D_{CO_2} < D_{N_2} < D_{O_2} < D_{H_2}$$

This order is substantially contrary to the following order of the effective molecular diameters of the five gases [10,11]:

$$H_2 < O_2 < CO_2 < N_2 < CH_4$$

Only an abnormal phenomenon ( $D_{CO_2} < D_{N_2}$ ) was observed because  $CO_2$  exhibits smaller effective diameter than  $N_2$ . Similar relationship between the diffusivity and effective molecular diameter of the gases has been found for pure EC membrane at the upstream pressure of 2–10 bar [18]. Note that  $D_{CO_2}$  appears to be larger than  $D_{N_2}$  for the EC membrane at a higher upstream pressure of 20 bar and 25°C [18] or for the pure PVP membrane [10]. It may be concluded that the diffusivity of the gases through the PVP/EC blend membranes containing not more than 60 wt% PVP is mainly controlled by EC component at a low upstream pressure.

### 3.4. Gas solubility performance

The solubility versus blend composition plots at 25°C are shown in Fig. 8. The  $H_2$  solubility is much lower than those of other four gases in the membranes, leading much lower solubility selectivity of  $H_2$  over  $N_2$  of 0.75–0.55. One of reasons is that hydrogen has the weakest interaction with the blends. The greatest  $CO_2$  solubility and  $CO_2/CH_4$  solubility selectivity in the blend membranes are attributed to the relatively high solidification point and the strongest interacting of  $CO_2$  with the blend membranes.

Additionally, the solubilities of five gases through the blend membranes decrease monotonically and slowly with increasing PVP content from zero to 60 wt%. Although  $O_2/N_2$  and  $H_2/N_2$  solubility selectivities decrease slightly but the  $CO_2/CH_4$  solubility selectivity increases slightly with increasing PVP content, due to a much faster decrease in solubility of  $CH_4$  than  $CO_2$ , as shown in Fig. 8(b). These variations of solubility and its selectivity with blend composition are different from those of the permeability, diffusivity and their selectivities versus composition (Figs. 6 and 7). Experimental  $H_2$  solubility falls slightly below the line drawn on the semilogarithmic scale but the experimental solubilities for other four gases are slightly above the line. Addition of about 33 wt% of PVP to EC linearly decreases the solubilities of  $O_2$ ,  $N_2$ ,  $CO_2$ , and  $CH_4$  in the blend membranes, i.e. the gas solubilities become additive for



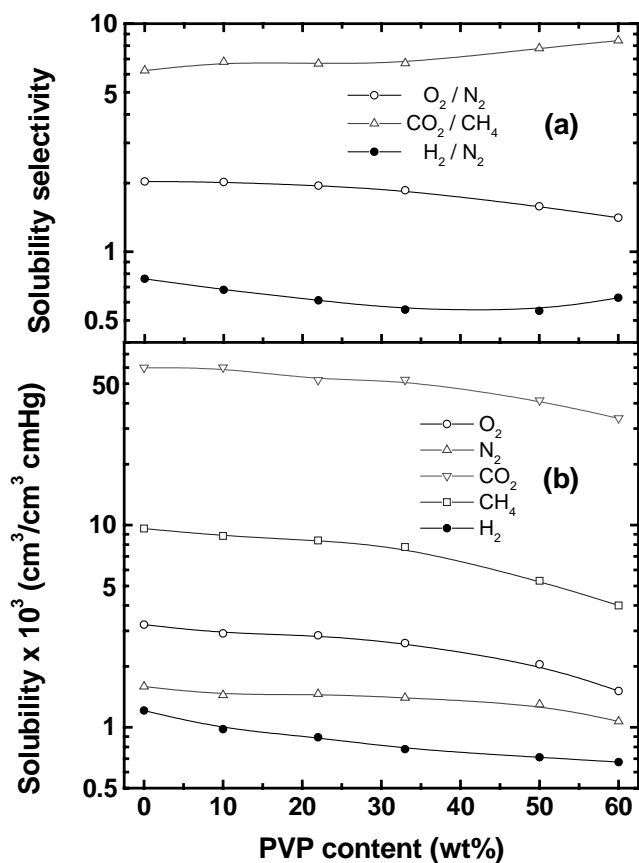


Fig. 8. The variation of solubility (b) and solubility selectivity (a) through the blend membranes of poly(4-vinylpyridine) (PVP)/ethyl cellulose (EC) with PVP content at 25°C and transmembrane pressure difference of 1–5 bar.

the blend component. Further addition of PVP to about 60 wt% gives a slightly apparent decrease in the solubilities of  $O_2$ ,  $N_2$ ,  $CO_2$ , and  $CH_4$  in the blend membranes.

### 3.5. Effect of temperature and upstream pressure on gas permselectivity

A typical relationship between gas permeability or permselectivity and reciprocal temperature for PVP/EC (50/50) blend membrane is shown in Fig. 9. The gas permeability through the membrane increased with an increase in temperature in a considered range of 25–55°C at a constant upstream pressure of 2 bar and is found to follow the Arrhenius law,  $P = P_0 \exp(-E_p/RT)$ . The activation energy ( $E_p$ ) values for the  $CO_2$ ,  $O_2$ ,  $H_2$ ,  $CH_4$ , and  $N_2$  permeation through the blend membrane calculated by the Arrhenius law are 4.2, 6.5, 8.0, 9.4, and 9.9 kJ/mol, respectively. These  $E_p$  values are lower than those of 4-vinylpyridine irradiation-grafted polymethylpentene membrane [17] but higher than those of pure EC membrane [18]. It was reported that the permeation activation energy through other polymer membranes follows almost the same trend with a variation of permeation gas [19], that is, the  $E_p$  value for  $CO_2$  is the

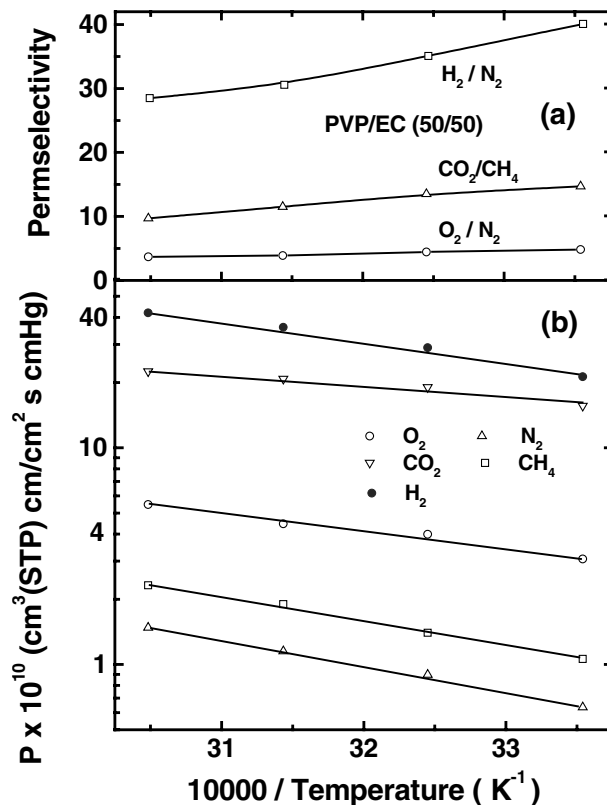


Fig. 9. The variation of permeability (b) and permselectivity (a) through the PVP/EC (50/50) blend membranes with reciprocal temperature at an upstream pressure of 2 bar.

smallest but the  $E_p$  values for  $N_2$  and  $CH_4$  are the largest. Additionally, as shown in Fig. 9(a), there is a linear relation between the permselectivity of three gas pairs and reciprocal temperature. The permselectivity increases with enhancing reciprocal temperature where  $P_{H_2}/P_{N_2}$  exhibits the strongest dependence on reciprocal temperature. This is the normal trend for most polymer membranes except for the liquid crystal membranes [3,5,6,8].

The oxygen permeation through the PVP/EC (60/40) blend membrane was studied with increasing upstream pressure from 2 to 20 bar at 35°C. The downstream pressure of the blend membrane increases rapidly after an initial time-lag from 36 to 170 s. The increase rate of downstream pressure with permeating time is strongly dependent on the upstream pressure. The permeability of five gases through the PVP/EC (50/50) blend membrane at 35°C is shown in Fig. 10 as a function of upstream pressure from 2 to 20 bar. The oxygen and methane permeability does not appear to be affected by pressure up to 20 bar, but the permeability of nitrogen and carbon dioxide decreased with increasing upstream pressure from 2 to 15 bar, demonstrating a typical transport behavior in common glassy polymers. Similar behavior was also observed for  $CO_2$  permeation through miscible glassy blend membranes of poly(butylene terephthalate)/a random copoly(bisphenol A- iso/terephthalates) [20] and polyethersulfone/polyhydroxyether [21].

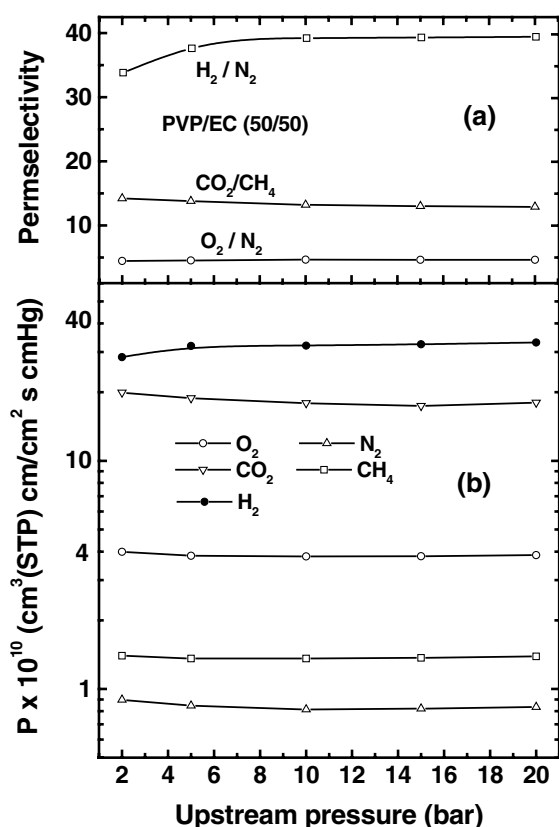


Fig. 10. The variation of permeability (b) and permeability selectivity (a) through the PVP/EC (50/50) blend membranes with upstream pressure at 35°C.

It should be noted that  $P_{H_2}$  slightly increased with increasing pressure from 2 to 10 bar, leading to an increase in  $P_{H_2}/P_{N_2}$  in the corresponding pressure range. Little pressure dependency is a general trend for glassy polymers in the absence of strong plasticization effects, whereas a slightly positive  $P_{H_2}$  dependence on upstream pressure could be because the pore blocking effect for hydrogen with the smallest molecular size among the five gases does not play such a significant role as the other four gases. A similar  $P_{H_2}$  — upstream pressure relationship has been reported for 4-vinylpyridine-grafted polymethylpentene membrane [17]. This is beneficial to the hydrogen/nitrogen separation because  $P_{H_2}$  and  $P_{H_2}/P_{N_2}$  can be increased concurrently with increasing upstream pressure.

#### 4. Conclusions

The PVP/EC blends are microscopically immiscible with a weak interaction between two phases. SEM observation reveals a randomly dispersed PVP spheroids in a continuous matrix of EC for PVP/EC blend membrane having less than 50 wt% PVP. When PVP of 50 wt% is added to EC and mixed by solution casting technique, EC appears to remain the continuous phase and interpenetrates into PVP phase. At the same time, phase inversion may occur, i.e. the PVP

component also begins to become a continuous phase. The fact that  $P_{O_2}$ ,  $P_{CO_2}$ , and  $P_{CH_4}$  decreased faster but  $P_{CO_2}/P_{CH_4}$  and  $P_{H_2}/P_{N_2}$  increased faster in a range of PVP content from 50 to 60 wt% is consistent with a continuous path formation of PVP phase. The permeability, diffusivity, and solubility of five gases including  $O_2$ ,  $N_2$ ,  $CO_2$ ,  $CH_4$ , and  $H_2$  through the PVP/EC blend membranes generally lay above a tie line constructed between the values for the pure PVP and pure EC using semilogarithmic coordinates. This behavior may be consistent with the fact that these blends show an increase in volume on solution mixing. The morphology and gas permselectivity reveal that the PVP/EC blends are quite attractive as gas separation membrane materials. Compared to the PVP homopolymer, PVP/EC blends exhibit improved mechanical properties, better membrane-forming ability, higher gas permeability, and much less expense, which are attributable to the presence of EC in the blend. As compared with pure EC, on the other hand, the blends have higher gas separation factor and also comparable gas permeability. This would appear to be general for all microscopically immiscible polymer blends and has important practical ramifications for applications, where high permselectivity is an important consideration.

#### Acknowledgements

The project was supported by (1) the National Natural Science Fund of China (29804008), (2) the Fund of Visiting Professor of Technical University of Berlin Germany, (3) the Fund of the University Key Teacher by Chinese Ministry of Education (GG-430-10247-1186), (4) the Phosphor Plan of Science Technology for Young Scientists of Shanghai China (98QE14027), (5) the State Key Laboratory for Modification of Chemical Fibers and Polymer Materials at Donghua University of China. (6) the Key Laboratory of Molecular Engineering of Polymers of China. Prof. Dr Xin-Gui Li is thankful to the Technical University of Berlin for the financial support of his research stay in Berlin and also thank Prof. Dr Zhi-Kang Xu at Zhejiang University China for his help in gas transport measurement.

#### References

- [1] Kapantaidakis GC, Kaldis SP, Sakellaropoulos GP, Chilra E, Loppinet B, Floudas G. *J Polym Sci, Part B* 1999;37:2788.
- [2] Kim MH, Kim JH, Kim CK, Kang YS, Park HC, Won JO. *J Polym Sci, Part B* 1999;37:2950.
- [3] Huang M-R, Li X-G, Lin G. *Sep Sci Technol* 1995;30:449.
- [4] Li X-G, Huang M-R, Lin G, Yang P-C. *Colloid Polym Sci* 1995;273:772.
- [5] Li X-G, Huang M-R, Lin G. *J Membr Sci* 1996;116:143.
- [6] Huang M-R, Li X-G. *Gas Sep Purifi* 1995;9:87.
- [7] Li X-G, Huang M-R. *J Appl Polym Sci* 1997;66:2139.
- [8] Li X-G, Huang M-R, Hu L, Lin G, Yang P-C. *Eur Polym J* 1999;35:157.
- [9] Park C, Jo WH, Park HC, Kang YS. *Polymer* 2000;41:1765.
- [10] Shieh J-J, Chung TS. *J Polym Sci, Part B* 1999;37:2851.

- [11] Kresse I, Usenko A, Springer J, Privalko V. *J Polym Sci, Part B* 1999;37:2183.
- [12] Muruganandam N, Paul DR. *J Polym Sci, Polym Phys Ed* 1987;25:2315.
- [13] Petropoulos JH. *J Polym Sci, Polym Phys Ed* 1985;23:1309.
- [14] Ranby BG. *J Polym Sci Symp* 1975;51:89.
- [15] Masi P, Paul DR, Barlow JW. *J Polym Sci, Polym Phys Ed* 1982;20:15.
- [16] Morel G, Paul DR. *J Membr Sci* 1982;10:273.
- [17] Lai JY, Wei SL. *J Appl Polym Sci* 1986;32:5763.
- [18] Li X-G, Kresse I, Xu Z-K, Springer J. *Polymer* 2001;42:6791.
- [19] Costello LM, Koros WJ. *J Polym Sci, Part B* 1995;33:135.
- [20] Chin S, Gaskins T, Durning CJ. *J Polym Sci, Part B* 1996;34:2689.
- [21] Reimers MJ, Barbari TA. *J Polym Sci, Part B* 1994;32:131.